International Journal of the Physical Sciences Vol. 7(5), pp. 797 - 804, 30 January, 2012
Available online at http://www.academicjournals.org/IJPS
DOI: 10.5897/IJPS11.1701
ISSN 1992 - 1950 © 2012 Academic Journals

Full Length Research Paper

Speckle noise reduction methods in cardiac cycles

Simona Moldovanu[1], Luminita Moraru[1]*, Essaid Zerrad[2] and Anjan Biswas[3]

[1]Department of Chemistry, Physics and Environment, University Dunarea de Jos of Galati, 111 Domneasca ST, 800201, Galati, Romania.
[2]Department of Physics and Pre-Engineering, Delaware State University Dover, DE 19901-2277 USA.
[3]Department of Mathematical Sciences, Delaware State University Dover, DE 19901-2277 USA.

Accepted 06 January, 2012

Speckle noise is omnipresent in imagistic and is an important problem in imagistic because it is the main source of noise in echography and echocardiography images and it should be reduced without affecting the image features. In spite of wider study dealing to speckle noise removal, until now there is no comprehensive method that covers all the constraints. In this study, three techniques were used for despeckling in echocardiography images along cardiac cycles for apical two chamber view (A2C), apical four chamber view (A4C), parasternal long axis view (LAX), and parasternal short axis view (SAX) and their results were compared. To assess the performances of filters, the correlation coefficient (CoC) was used. Following this analysis, the proper filtering method is recommended.

Key words: Echocardiography images, despeckling, correlation coefficient.

INTRODUCTION

The incidence of the heart diseases is continually increasing worldwide and it is compulsory to establish new automatically ways to allow a fast, correctly and objectively diagnosis of myocardial function.

Echocardiography as a B-mode ultrasound imaging modality contributes to observe the clinical manifestations and features of the heart and to assess the vulnerability of the heart muscle. Moreover, it provides efficacious information about the heart health and function. Because it is a cheap and fast method, the echocardiography technique becomes a common functional way to diagnose and describe most heart problems. In echocardiography, the reflected sound pulses around and in the heart are processed into images (Edward et al., 2010). Echocardiography images may show function heart valves abnormalities or heart tissue damages after acute myocardial infarction. They present low texture quality of images caused, in principal, by noise, low frequency and small dimension of the walls. Unfortunately, echocardiography images are affected by speckles which represent the dominant source of noise in ultrasound imaging; so the ultrasound investigation of the myocardial function is a challenge because any visual assessment of heart is subjective and requires extensive training. In this context, the main purpose of the despeckling action in medical ultrasound imaging is to improve the human interpretation of the ultrasound images. The speckle suppression improves the speed and accuracy of automatic and semiautomatic segmentation and registration (Narayanan and Wahidabanu, 2009).

Adam et al. (2006) showed that the speckle noise is a multiplicative noise, it leads to granular appearance, degrades both the contrast and resolution of the images and its suppression ensured that the features of interest for diagnosis are not lost.

Generally, the noise in any kind of images is defined as a random signal that obscures many details in a true image. Noise modifies the intensity and distribution of the pixels across the entire image and makes the image inconsistent with reality. The electrical parasites signals generated by the electronic components of the digital devices are the main sources of noise. There are many different distributions that characterize the noise into image such as: Gaussian distribution, salt and pepper noise, Rayleigh distribution, Maxwell distribution etc.

In order to overcome the speckle problem, many speckle reduction methods were implemented as single scale spatial filtering and multiscale method. The first

*Corresponding author. E-mail: luminita.moraru@ugal.ro.

category includes the Kaun and Lee filters (Kaun et al.,1987), Frost filter (Frost et al.,1982), mean filter (Frery et al., 1997), median filter (Loupas et al.,1998) and Gaussian filter (Malpica et al., 2005) while the wavelet (Nicolae et al., 2010) and pyramid (Aiazzi et al.,1998) techniques belong to the second category. Another approach of image filtering techniques covered the spatial domain (by direct manipulation of image pixels) or the frequency domain (by using the manipulating of the low or high frequencies from decomposed image). Some examples of filtering in spatial domain are the linear filter (based on the convolution of the image and a filter mask) and the non-linear filter (median filter). We approach the problem of speckle noise removal from echocardiography images as a first, but necessary, step in our currently attempt to extract some important features as the endocardial and epicardial boundaries, and the myocardial centreline - which are potentially helpful in any subsequent processing or in assessment of left ventricular diastolic and systolic function and detailed cavity geometry and position of mitral valve. Thus, we analyze the efficiency of several speckle noise reduction/ removal process in echocardiography images which belong to a cardiac cycle. These methods are Wiener filter, median filter and Gaussian filter. This despeckling technique is necessary for improving the human inter-pretation of echocardiography images and it improves the speed and accuracy of automatic and semiautomatic segmentation of images.

Usually, the performances assessment of these methods are done using the correlation coefficient (CoC), contrast to noise ratio (CNR), peak signal to noise ratio (PSNR) or structural similarity index (SSI) parameters (Narayanan and Wahidabanu, 2009).

Our approach intends to test three different de-noising filters on cardiac cycle and to calculate the CoC from each of two echocardiographic sequences, end-diastole and end-systole frames.

CARDIAC CYCLE

A cardiac cycle comprises all events that exist in the period of a heart. One cycle has two major separate stages: diastole and systole. According to Klabunde (2005), the cardiac cycle is divided into seven phases. The first phase is ‘atrial contraction’. The second phase is ‘isovolumetric contraction’ which begins with atrio-ventricular valve closures and ends with the opening of the aortic and pulmonic valves. During this phase, the ventricular volume is at its maximum and the phase is named the end-diastolic volume. The third phase is ‘rapid ejection’; in this phase blood flows into the aorta and pulmonary arteries rapidly. The fourth phase is ‘reduced ejection’. The fifth phase is ‘isovolumetric relaxation’ that begins with the closure of aortic and pulmonic valves and ends with opening of atrioventricular valves. Since all valves are closed, during this phase the ventricular volumes remain constant but their pressures decrease. This volume is called end-systolic volume. The sixth phase is ‘rapid filling’ in which the atrioventricular valves open and ventricular rapid filling begins. Finally, the seventh phase is ‘reduced filling’ (Klabunde, 2005).

MATHEMATICAL DESCRIPTION

The basic idea in digital image filtering is to post-process an image using the pixel intensity remapping. The noise into image has various sources and it is demand to use the appropriate model for robust image restoration. Noise may be additive and it can be expressed as $g(x,y)=f(x,y)+n(x,y)$ where $f(x,y)$ is the original 2D signal (image), n is the noise contribution, and g is the corrupted image. The noise can also be multiplicative, namely $g(x,y)=f(x,y)n(x,y)$. From another point of view, noise may be highly correlated or completely uncorrelated. If the noise is established as being highly structured, then defects in the manufacturing process of the detector are indicated as being the possible source. One possible solution for noise reduction is to replace defaulting pixels with the average of its neighbours. Simultaneously, the ultrasound devices themselves usually perform a pre-processing of the acquired data including even logarithmic compression. Thus, in the displayed medical ultrasound images, the noise differs significantly from often assumed multiplicative method (Moldovanu and Moraru, 2010).

Wiener filter

The Wiener filter is commonly used to restore linearly degraded images, and it is based on minimum squared error (MSE). At the same time, it is an optimal linear filter for stationary environment in the sense of producing the best estimate of the signal. Here, the word ‘‘optimal’’ is used in the sense of minimum mean-square error. The assumption underlying the theoretical construction of the Wiener filter claims that the power spectrum of the ideal image and the noise are known. Mohamed et al. (2007) showed that the Wiener filter allows estimating an original image as being the solution of the linear MSE problem when a measured image is handled. This estimation can be expressed as a convolution of the measured signal with a time invariant filter. The frequency response of the non-causal Wiener filter (when a large amount of data is required so it is not suited for real-time applications) is

$$H(w)=\frac{P_s(w)}{P_s(w)+P_N(w)},$$

where $P_s(w)$ and $P_N(w)$ represent the power spectral density of the true signal and the noise, respectively (Mohamed et al., 2007).

Median filter

The following reasons make the linear filters so attractive: they possess useful algebraic properties; their embedded operations are easily understood; via Fourier transform, they have direct relations to frequency representation and their statistical properties are well digested.

Median filtering was introduced by Tukey to smooth economic time series (Doughetery, 1994). The 1D filter can be implemented by sliding a "window" (that surrounding the pixels in discussion) over the entire image. The result of the median operation over the pixels into the window is the filter output. We let *N* denote the window size and because it is necessary to be an odd integer, we write $N = 2k + 1$. The mathematical expression of the median filter of length *N* can be expressed as (Doughetery and Astola, 1994) follows:

$$y(n) = \text{MED}\,[\,x(n-k), .., x(n), ..., x(n+k)] \quad (1)$$

here *x(n)* and *y(n)* are the input and output sequence. This is often called the running median. In image processing, the median filtering is usually applied by moving a square or cross-shaped window and choosing the median of the pixel value within the current window output (Moldovanu and Moraru, 2010).

Gaussian filter

In our attempt to handle the problem of blurring structures, we use the Gaussian filter for removing shadow and smoothing image. In a 2D space, the kernel can be defined as:

$$G_\sigma(x, y) = \frac{1}{2\pi\sigma^2} e^{-\frac{x^2+y^2}{2\sigma^2}} \quad (2)$$

where σ^2 is the variance of the Gaussian distribution function (Malpica et al., 2005).

Equation 2 shows a normal probability distribution and it is used to define a Gaussian filter that actually describes the probability density function having a mean of zero (that is, it is centered on the line *x*=0) and variance σ .

The Gaussian filter is the better solution of narrow low pass filters of the image. Among the advantage of this filter we mention: it is an effective averaging filters and it computes a weighted average of the values inside the local window.

Correlation coefficient

The CoC is a method that employs tracking and image registration techniques and it allows to accurately estimating changes into images. It estimates the similarity between the original and demonised images. The CoC between two image A_{mn} and B_{mn} is:

$$r = \left(\sum_m \sum_n \left(A_{mn} - \bar{A} \right) \left(B_{mn} - \bar{B} \right) \right) \Bigg/ \sqrt{\left(\sum_m \sum_n \left(A_{mn} - \bar{A^2} \right) \left(B_{mn} - \bar{B^2} \right) \right)} \quad (3)$$

where $\bar{A}$ and $\bar{B}$ are average or mean of image matrix elements (Narayanan and Wahidabanu, 2009).

EXPERIMENTAL

In this study, the hardware experiment environment was Intel (R) Core (TM) 2 Duo CPU T 5900, 2.20 with 3G RAM, and the programming environment is the MATLAB R2009a. The images used for the analysis are acquired from scanning systems, VIVID E9 and GE HORTEN MOK WAY using curvilinear probe with transducer frequency of 3.5 MHz. The echocardiography images of the heart used in this research were all captured from the same machine and then digitized with 512 x 524 pixels and 256 grey-level resolutions.

The accurate detection of the end-diastole and end-systole frames of echocardiography images is very important for further analysis of various features related to heart motion abnormalities. There are real difficulties in dealing to biomedical processing information due to variability of the signals and the biases induce by artefacts. Apart from the engineering applications where only certain procedures that are elaborated under very specific assumptions are necessary, in the case of biomedical signals, the relevant and pertinent information that are necessary are found by a deviation of certain signal features from the normal values. An additional aspect of the processing of biomedical images process deals with its complex approach when one or more combination of features (either localized temporally or spatially) are handled to provide the required information. The filtering operation is an active process in designing versatile and robust analysis methods.

The cardiac motion abnormalities characterization is based on the correct detection of the end-systole and end-diastole frames of echocardiography image sequences (Jacob et al., 2001, 2002; Barcaro et al., 2008; Beymer et al., 2009; Giachetti, 1998; Kachenoura et al., 2007). For heart function assessment, the high quality of these frames is needed to facilitate the measurement of the fundamental parameters. The speckle noise removal is the first step in feasible detection of the end-diastole and end-systole frames and for further automatic calculation of various features. Currently, the physician determinates the end-systole frame and end-diastole frame mostly visualize through slow animation of loops with a trackball. However, in echocardiography imaging, the frames from a video sequence of a particular patient may vary due to a small number of factors such as deformation caused by the patient's heartbeat, imaging geometry and noise.

RESULTS AND DISCUSSION

Numerous despeckling techniques have been proposed and they utilized the same basic adaptive filtering concept. The differences of the various despeckling methods are the various ways used to choose how to smooth and/or the diverse criteria used to determine the degree of

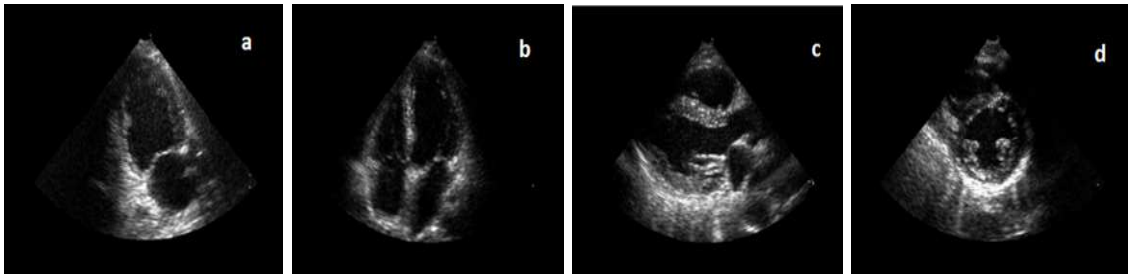

Figure 1. Four different ultrasound views of the heart: a, Apical two chamber view; b, apical four chamber view; c, parasternal long axis view; d, parasternal short axis view.

Table 1. The values of CoC between consecutive frames for four views as SAX, A2C, LAX and A4C without filtering.

Frame number	SAX	A2C	LAX	A4C
1				
2	0.975	0.978	0.974	0.978
3	0.980	0.978	0.975	0.981
4	0.981	0.981	0.977	0.984
5	0.971	0.981	0.979	0.978
6	0.977	0.978	0.946	0.971
7	0.976	0.978	0.972	0.943
8	0.970	0.971	0.964	0.965
9	0.979	0.971	0.965	0.971
10	0.978	0.973	0.971	0.973
11	0.980	0.973	0.974	0.976
12	0.976	0.983	0.977	0.979
13	0.983	0.983	0.979	0.974
14	0.981	0.981	0.972	0.969
15	0.974	0.981	0.966	0.967
16	0.978	0.970	0.969	0.971

of smoothing. We looked to evaluate the despeckling performance of median and Gaussian filters. To implement our study, the image sequences were visually analyzed by an experienced echo cardiologist and the end-systolic and end-diastolic frames were determined. In Figure 1, typical images for all usually type of views of the heart cavity are shown. The CoC is applied between two consequently frames for all views [(parasternal short axis view (SAX), apical two chamber view (A2C), parasternal long axis view (LAX) and apical four chamber view (A4C)]. In this study, CoC was computed for all frames of one cardiac cycle. In a first step, the CoC was extracted from the original US images and the results are shown in Table 1. In the second step, CoC was computed for the filtrated US image using the median filter, filter Wiener and Gaussian filter.

Three different filtering methods (median, Wiener, Gaussian) were applied. The obtained performances of the measurements using these filters are shown in Tables 2, 3 and 4, respectively.

The Wiener filter was successfully implemented and tested in despeckled phantom and *in vivo* US images by Nadernejad et al. (2009). They were concluded that “the Wiener filter can improve the image qualities well and simulated power spectrum of speckle can be applied on many situations”. The median filters are also utilized for despeckling due to their robustness against impulsive type noise and edge preserving characteristics (Narayanan and Wahidabanu, 2009).

These three filters applied on echocardiography have been confirmed their robustness as the values of CoC obtained after filtering operation are close to 1.

For SAX, A2C, LAX and A4C views and for each filter, the average values of CoCs were computed. The obtained values are shown in Table 5 and interpreted in Figure 2. It showed the variation of CoC, frames by frames, between end- systole and end diastole, for four ultrasound views of the heart.

Table 2. The values of CoC between consecutive frames for four views SAX, A2C, LAX and A4C, for median filtering.

Frame number	SAX	A2C	LAX	A4C
1				
2	0.982	0.985	0.982	0.983
3				
4	0.986	0.986	0.981	0.984
5				
6	0.986	0.989	0.982	0.986
7				
8	0.979	0.985	0.985	0.988
9				
10	0.983	0.982	0.985	0.983
11				
12	0.982	0.988	0.981	0.977
13				
14	0.978	0.977	0.982	0.969
15				
16	0.985	0.977	0.971	0.971
	0.984	0.978	0.972	0.982
	0.986	0.985	0.977	0.978
	0.983	0.987	0.979	0.981
	0.988	0.986	0.981	0.983
	0.981	0.980	0.983	0.979
	0.984	0.979	0.977	0.974
	0.984	0.984	0.971	0.972

Table 3. The values of CoC between consecutive frames for four views as SAX, A2C, LAX and A4C for Wiener filtering.

Frame number	SAX	A2C	LAX	A4C
1				
2	0.988	0.989	0.986	0.983
3				
4	0.991	0.991	0.987	0.989
5				
6	0.990	0.992	0.988	0.980
7				
8	0.985	0.998	0.990	0.992
9				
10	0.988	0.987	0.989	0.988
11				
12	0.988	0.982	0.987	0.975
13				
14	0.985	0.981	0.984	0.977
15				
16	0.991	0.983	0.977	0.982
	0.989	0.989	0.977	0.983
	0.991	0.989	0.983	0.986
	0.989	0.989	0.985	0.987
	0.991	0.983	0.986	0.984
	0.987	0.988	0.988	0.979
	0989	0.978	0.982	0.978
	0.989	0.979	0.977	0.980
			0.980	

Taking into account the obtained data and the comparison between end-diastolic and end-systolic frames shown in Tables 1, 2, 3 and 4 and the evolution the average values of CoC we can conclude that significant differences could be found between the parameters of the echocardiography heart images without filter and those of processed images using Wiener, median and Gaussian filters. In the same time, there are insignificant differences between the average values of the CoC for filtered images. The diagram presented in Figure 2 shows the better results of Wiener filter for SAX view and of median and Wiener filters for A2C view; Wiener and Gaussian filters have suitable results for LAX view and median and Gaussian filters for A4C view. The surfaces of the diagram shown in Figure 3 indicate that the CoC is predominating in range [0.980; 0.985] meaning that all the filters have generated the values in this interval. Moreover, the higher values are in range of

Table 4. The values of CoC between consecutive frames for four views as SAX, A2C, LAX and A4C for Gaussian filtering with $\sigma = 0.5$.

Frame number	SAX		A2C		LAX		A4C	
1	0.9815		0.9790		0.9845		0.9835	
2		0.9821		0.9863		0.9806		0.9786
3	0.9794		0.9796		0.9703		0.9720	
4		0.9814		0.9747		0.9729		0.9762
5	0.9815		0.9786		0.9746		0.9763	
6		0.9804		0.9784		0.9760		0.9767
7	0.9804		0.9782		0.9777		0.9780	
8		0.9815		0.9788		0.9775		0.9798
9	0.9826		0.9804		0.9777		0.9818	
10		0.9749		0.9819		0.9795		0.9825
11	0.9832		0.9835		0.9812		0.9847	
12		0.9829		0.9862		0.9833		0.9877
13	0.9834		0.9876		0.9814		0.9835	
14		0.9766		0.9815		0.9814		0.9789
15	0.9856		0.9802		0.9758		0.9681	
16								

Table 5. Average of CoC values according to four ultrasound views of the heart.

	SAX	A2C	LAX	A4C
Without filter	0.98	0.9795	0.97	0.9725
Median filter	0.98	0.985	0.982	0.983
Wiener filter	0.99	0.9835	0.9845	0.9805
Gaussian filter	0.983	0.9805	0.985	0.983

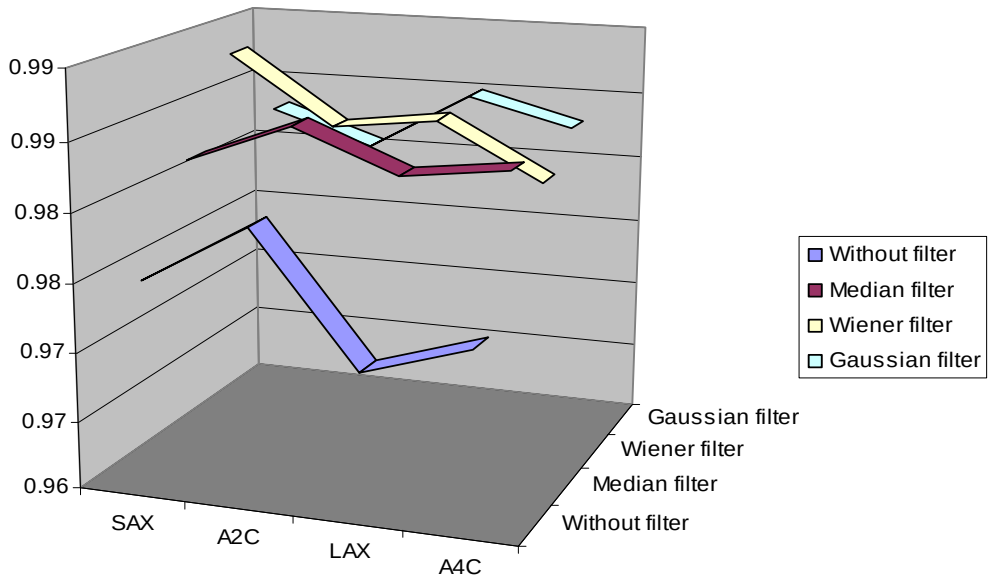

Figure 2. Evolution of CoC values for four ultrasound views of the heart healthy patients.

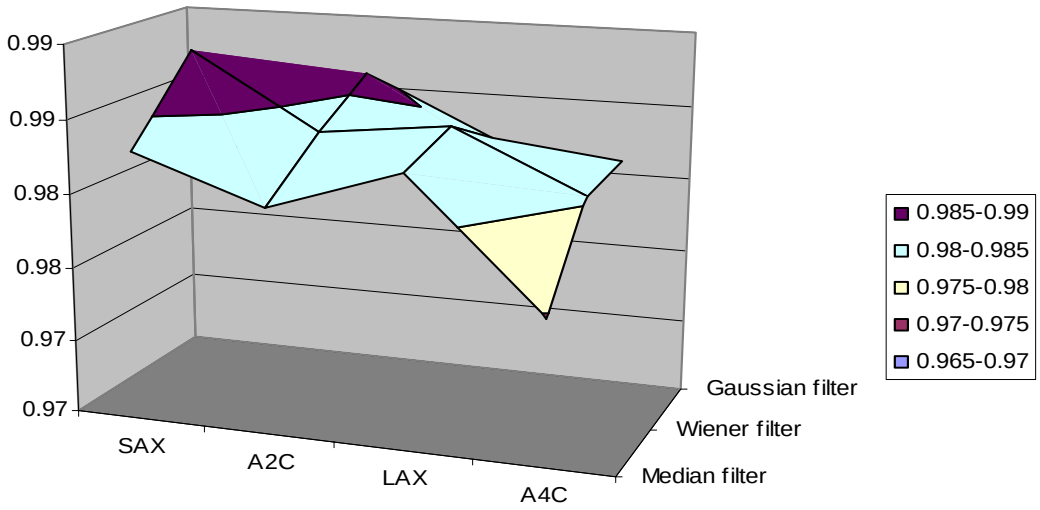

Figure 3. Predominate values of CoC in each view way.

[0.985; 0.990] and most of them belong to SAX view.

This study is a challenge to extract important clinical information in accordance to the view ways of the echocardiography images and to select the proper filtering methods. The presented method can be useful for further processing in echocardiography.

CONCLUSION

The filtering method and speckle model are important in the design of despeckling methods and they differ from application to application. The current study demonstrated that noise in cardiac cycle persists between two consecutive frames regardless of what kind of views of the heart cavity are used. As expected, subsequently the filtering operation the image quality is improved. Moreover, our study confirmed through the CoC values that the Weiner filter is more robust in de-noising the cardiac cycle and it is suitable for removing the noise. Other filtering methods may also be studied in order to make an exhaustive comparison between these filters used on a variety of US images.

ACKNOWLEDGEMENTS

The author Simona Moldovanu would like to thank the Project SOP HRD-EFICIENT 61445/2009 of Dunarea de Jos University of Galati, Romania for the support. The research work of the third and fourth authors (Essaid Zerrad and Anjan Biswas) was fully supported by Army Research Office (ARO) and Air Force Office of Scientific Research (AFOSR) under the award number: W54428-RT-ISP and this support is thankfully recognized.

REFERENCES

Adam D, Beilin-Nissan S, Friedman Z, Behar V (2006). The combined effect of spatial compounding and nonlinear filtering on the speckle reduction in ultrasound images. Ultrasonics, 44(2): 166–81.

Aiazzi B, Alparone L, Baronti S, Lotti F (1998). Multiresolution local statistics speckle filtering based on a ratio laplacian pyramid. IEEE Trans. Geosci. Remote Sens., 36(5): 1466-1476.

Barcaro U, Moroni D, Salvetti O (2008). Automatic computation of left ventricle ejection fraction from dynamic ultrasound images. Pattern Recogn. Image Anal., 18(2): 351–358.

Beymer D, Syeda-Mahmood T, Amir A, Wang F, Adelman S (2009). Automatic estimation of left ventricular dysfunction from echocardiogram videos. In: Proc. IEEE Computer Society Workshop on Mathematical Methods in Biomedical Image Analysis, MMBIA, Miami, SUA, pp. 723-730.

Doughetery ER (1994). Digital Image Processing Methods. Marcel Dekker, New York, pp. 7-23.

Doughetery ER, Astola J (1994). An introduction to nonlinear Image Processing. SPIE Press, Bellingham, pp. 17-37.

Edward J, Blair A, Rigolin V (2010). Echocardiography. In: Goldberger J, Ng J (eds) Practical Signal and Image Processing in Clinical Cardiology. Springer, Chicago Ilinois, pp. 187-218.

Frery AC, Müller HJ, Yanasse CCF, Sant'Anna SJS (1997). A model for extremely heterogeneous clutter. IEEE Trans. Geosc. Rem. Sens., 35(3): 648-659.

Frost VS, Stiles JA, Shanmugan KS, Holtzman JC (1982). A model for radar images and its application to adoptive digital filtering for multiplicative noise. IEEE Trans. Pattern Anal. Machine Intell., 4(2): 157-166.

Giachetti A (1998). On-line analysis of echocardiographic image sequence. Med. Image Anal., 2(3): 261–284.

Jacob G, Noble JA, Kelion AD, Banning AP (2001). Quantitative regional analysis of myocardial wall motion. Ultrasound Med. Biol., 27(6): 773–784.

Jacob G, Noble JA, Behrenbruch C, Kelion AD, Banning AP (2002). A shape-space-based approach to tracking myocardial borders and quantifying regional left-ventricular function applied in echocardiography. IEEE Trans. Med. Imag., 21(3): 226–38.

Kachenoura N, Delouche A, Herment A, Frouin F, Diebold B (2007). Automatic detection of end systole within a sequence of left ventricular echocardiographic images using autocorrelation and mitral valve motion detection. In: Proc. Int. Conf. on IEEE EMBS Annual International Conference, Lyon, France, pp. 4504–4507.

Kaun DT, Sawchuk AA, Strand TC, Chavel P (1987). Adoptive restoration

of images with speckle. IEEE Trans. Acoust. Speech Signal Process. ASSP- 35: 373-383.
Klabunde RE (2005). Cardiovascular Physiology Concepts. Lippincott Williams & Wilkins, Philadelphia, pp. 21-52.
Loupas T, McDicken WN, Allan PL (1998). An adaptive weighted median filter speckle suppression in medical ultrasound images. IEEE Trans. Circuits Sys., 36(1): 129-135.
Malpica N, Garamendi JF, Desco M, Schiavi E (2005). Endocardial Tracking in Contrast Echocardiography Using Optical Flow. In: Oliveria JL, Maojo V, Martin-Sanchez F, Pereira AS (eds), Biological and Medical Data Analysis, Proceedings of the 6th International Symposium, Aveiro, Portugal, pp. 61-68.
Mohamed M, Abou-Chadi F, Ouda B (2007). Denoising Functional MRI: A Comparative Study of Denoising Techniques (2D). In: Kim SI, Suk ST (eds), Imaging the Future Medicine, Proceedings of the World Congress on Medical Physics and Biomedical Engineering: IFMBE, Seoul, Korea, pp. 913-920.
Moldovanu S, Moraru L (2010). Mass Detection and Classification in Breast Ultrasound Image Using k-means Clustering Algorithm. In: Gaiceanu M (eds), ISEEE, Proceedings of the 3rd International Symposium on Electrical and Electronics Engineering, Galati, pp. 197-201.
Nadernejad E, Karami MR, Sharifzadeh S, Heidari M (2009). Despeckle Filtering in Medical Ultrasound Imaging. Contemporary Eng. Sci., 2(1-4): 17–36.
Narayanan SK, Wahidabanu RSD (2009). A View on Despeckling in Ultrasound Imaging. Int. J. Signal Process. Image Process. Pattern Recognition, 2(3): 85-98.
Nicolae MC, Moraru L, Onose L (2010). Comparative Approach Speckle Reduction in Medical Ultrasound. Rom. J. Biophys., 20(1): 13-21.